

# Effect of spin injection from colossal magnetoresistance material into superconducting thin film of $\text{YBa}_2\text{Cu}_3\text{O}_{7-\delta}$

T.B. Hjelmeland  
Department of Physics,  
University of Oslo, P.O.Box 1048, Blindern, 0316  
Oslo, Norway  
[t.b.hjelmeland@fys.uio.no](mailto:t.b.hjelmeland@fys.uio.no)

Y. Volkov  
Kiev-Pechersk Lyceum 171  
Leipzig street 11A, 01015  
Kiev, Ukraine  
[veg2001@gmail.com](mailto:veg2001@gmail.com)

P. Mikheenko\*  
Department of Physics,  
University of Oslo, P.O.Box 1048, Blindern, 0316  
Oslo, Norway  
[\\*pavlo.mikheenko@fys.uio.no](mailto:*pavlo.mikheenko@fys.uio.no)

**Abstract**— By specific design of the sample, in which  $\text{SrTiO}_3$  substrate is fully covered by a thin film of the colossal magnetoresistive material  $\text{La}_{0.67}\text{Ca}_{0.33}\text{MnO}_3$  (LCMO) and the latter is partially covered by high-temperature superconductor  $\text{YBa}_2\text{Cu}_3\text{O}_{7-\delta}$  (YBCO), and by using multiple current and voltage contacts, direct evidence of spin injection from LCMO to YBCO is obtained. It is found that spin-polarized electrons injected from LCMO strongly influence not only superconducting, but also normal state of YBCO. The effect of deposition conditions of LCMO and YBCO and the quality of the interface on the spin injection efficiency is clarified. A surprising peak in the temperature dependence of resistance seen on ex-situ sample is explained as combination of two effects: strong influence of spin-polarized electrons on superconductor just below its critical temperature and the interface-controlled shift of Curie temperature of LCMO to low temperatures. Considering expected use of LCMO and YBCO in composite quantum computation circuits, a possibility of their combination with another advanced quantum material, graphene, is explored.

**Keywords**—high temperature superconductor; colossal magnetoresistance material; spin injection; nano-magnetism; graphene.

## I. INTRODUCTION

With advance of superconducting quantum computing [1], there is renewed interest to higher-temperature superconductors in combination with spin-polarized materials [2], which is stimulated by the attempts to confine quantum processing on nanometer scale making computers more compact, and extend their operation to higher temperatures [3]. Graphene [4] is another important material that demonstrates quantum behaviour even at room temperature. Merging spin-polarized materials, superconductors and

graphene would lead to novel quantum devices with enhanced performance and functionality.

Two particular materials: spin-polarized  $\text{La}_{0.67}\text{Ca}_{0.33}\text{MnO}_3$  (LCMO) and high-temperature superconductor  $\text{YBa}_2\text{Cu}_3\text{O}_{7-\delta}$  (YBCO) are of special interest [5,6], as they have similar crystal lattice and can be prepared epitaxially on top of each other. There are multiple investigations of these compounds and their effect on each other, see, for example [5-8]. However, simple experiments showing where their interaction is strongest are needed and combinations of these materials with graphene should be explored.

LCMO and YBCO are delicate compounds. Small changes in their chemical composition, especially oxygen content, presence of impurities or diffusion of elements through interface, when they are prepared together, can produce unexpected effects, like appearance of stripy magnetic structure and resistance peak below critical temperature of superconductor [9].

In this paper, using specific design of LCMO/YBCO bilayer, we clarify nature of the resistance peak, demonstrate effect of spin injection on superconducting and normal state of YBCO and explore possibility of combining LCMO and YBCO with graphene.

## II. EXPERIMENTAL

A bilayer thin-film structure containing LCMO and YBCO was epitaxially grown by pulsed laser deposition on  $\text{SrTiO}_3$  (STO) substrate. First, the  $5 \times 10\text{-mm}^2$  substrate was fully covered by a 100-nm thick layer of LCMO. After that, using

mask, about half of LCMO layer was covered by a 200-nm layer of YBCO, as is shown in Fig. 1. Six indium contacts were attached to the sample, whose position is also shown on the figure. Some of them were attached to YBCO and some to LCMO. These contacts allow large variety of measurements depending on which of them are used for passing current and which for measuring voltage. For example, using as current contacts  $I_1$  and  $I_3$ , charge carriers are forced to flow from LCMO to YBCO, whereas the choice of current contacts  $I_1, I_2$  confines the carriers mainly to YBCO. At a defined current flow, a variety of potential measurements could be done using different potential contacts.

Before attaching contacts, sample was thoroughly investigated, as in [9], by magneto-optical imaging and scanning electron microscopy to insure desirable properties of both materials. In this paper, however, focus is on electrical transport measurements, for which a constant voltage load technique is chosen. The investigation mainly deals with the temperature dependence of the resistance for different parts of the sample.

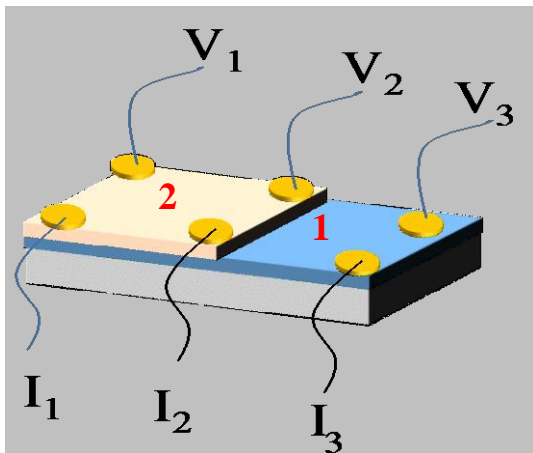


Figure 1: Schematic presentation of the measured sample. The number 1 marks a 100 nm thick layer of LCMO deposited on STO substrate, below. The 200-nm YBCO layer deposited above LCMO, is marked as 2. Several contacts are attached to the sample. Some of them are used for passing current ( $I_{1,3}$ ) and some for measuring voltage ( $V_{1,3}$ ).

The sample with attached wires was mounted on a thermally insulated rod, whose temperature was changed by immersing it to, or retracting it from, liquid nitrogen or liquid helium. This was done slowly to avoid appearance of hysteresis on the temperature dependence of resistance.

The constant voltage load to the measuring circuit is simple technique that does not require electronic adjustment of the current due to change of the resistance of the sample in the process of changing the temperature. Its disadvantage is that current does not remain constant during the measurement. However, registering current separately allows obtaining additional information about the sample.

### III. RESULTS AND DISCUSSION

Typical temperature dependence of resistance of the sample with current flowing through contacts  $I_1$  and  $I_3$  and voltage measured by contacts  $V_1$  and  $V_3$  is shown in Fig. 2. It was recorded at fixed circuit load with voltage of 6 V. Both magnetic (main plot) and superconducting transition (inset) are clearly seen. The magnetic transition is displayed as sharp decrease in resistance at Curie temperature ( $T_{\text{Curie}}$ ) of about 250 K, typical for LCMO [5-8]. The superconducting transition (shown in the magnified part of the curve in the inset) takes place at temperature about 80 K, which is somewhat lower than critical temperature ( $T_c$ ) of optimally-doped YBCO. This indicates inter-diffusion between YBCO and LCMO, which is, again, typical for the growth of these compounds on top of each other without thin separating barrier in-between. After superconducting transition, at lower temperatures resistance is not zero because in this configuration there is a layer of normal LCMO connected in series with YBCO. The long tail below  $T_c$  comes from overlap of  $R(T)$  curves of superconducting and spin-polarized materials.

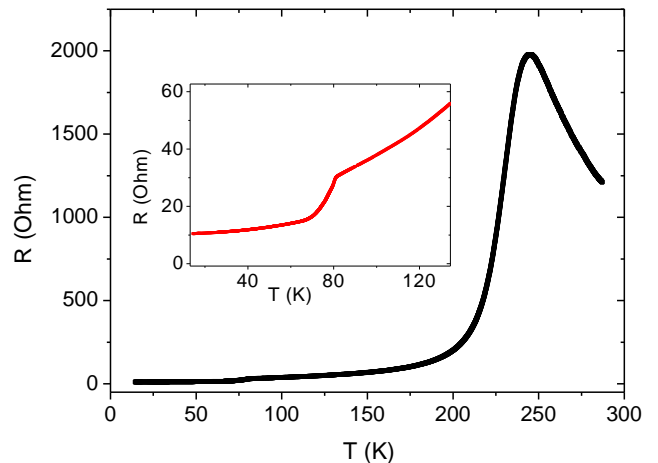


Figure 2: Temperature dependence of resistance of the sample in Fig. 1 with current flowing through contacts  $I_1$  and  $I_3$  and voltage measured by contacts  $V_1$  and  $V_3$ . The curve was recorded at the fixed circuit load with voltage of 6 V. Inset shows magnified part of the curve around the superconducting transition of YBCO.

Several curves, similar to that shown in Fig. 2, were recorded at different voltage loads. They also register two transitions with minor systematic variations between them. In the technique, current does not stay constant during temperature scans. Its change with temperature is shown in Fig. 3 for six voltage loads (see color legend in the inset) from 1 to 15 V. The curves in Fig. 3 can also be used to identify temperature of magnetic and superconducting transitions. Indeed, there is sharp increase in current when resistance of LCMO drops below  $T_{\text{Curie}}$  of about 250 K, and there is another increase in current when YBCO becomes superconducting. To demonstrate this, a magnified part of the curve at 6 V (green color) at temperatures around  $T_c$  is shown in Fig. 4.

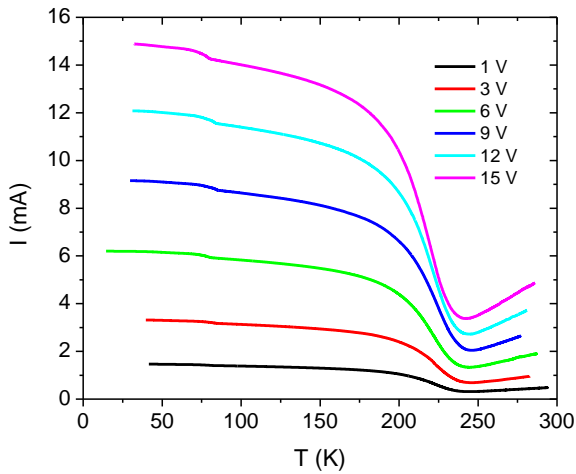


Figure 3: Temperature dependence of current at six constant voltage loads. Their values are shown in the legend in the inset.

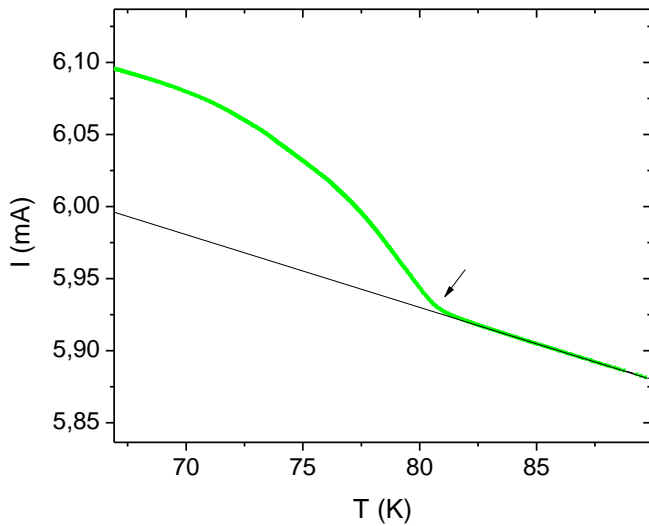


Figure 4: Magnified part of the curve at 6 V in Fig. 3 at temperatures around  $T_c$  of YBCO. A thin black line is shown for the guide of eye.

Analysis of the curves similar to those shown in Figs. 2-4 allows obtaining information about the sample as whole. The main advantage of the design in Fig. 1 is, however, ability to explore different parts of the sample at different paths for current, which can either be confined in one of the materials or flow between them.

In Fig. 5, temperature dependence of resistance is shown for the sample in Fig. 1 with current flowing, as in Figs. 2-4, between contacts  $I_1$  and  $I_3$ , but voltage measured between contacts  $V_1$  and  $V_2$  that are connected directly to YBCO. Two curves for limiting voltage loads of 1 and 15 V are shown.

Since in Fig. 5 mainly properties of YBCO are measured, resistance shows monotonous quasi-linear decrease with

decrease of temperature. Below superconducting transition, resistance is zero. This is typical  $R(T)$  curve for a YBCO with one exception: there is small but distinctive anomaly at Curie temperature of LCMO marked by small arrow.

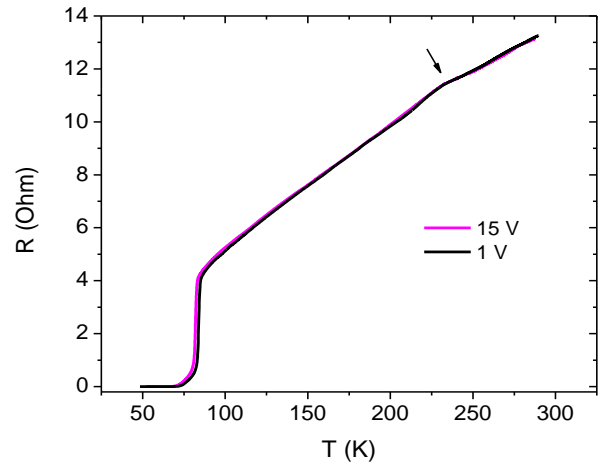
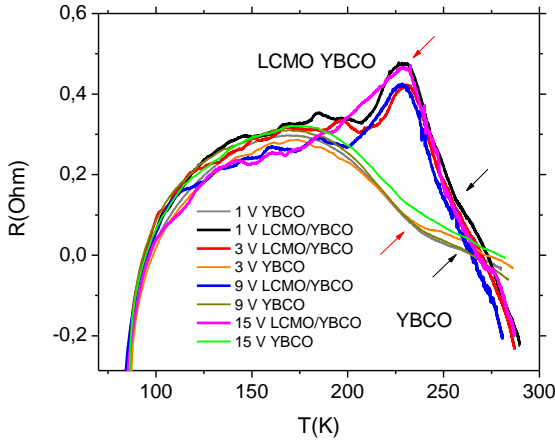


Figure 5: Temperature dependence of resistance for the sample in Fig. 1 with current flowing, as in Figs. 2-4, between contacts  $I_1$  and  $I_3$ , but voltage measured between contacts  $V_1$  and  $V_2$ . Two curves for voltage of 1 and 15 V are shown.

The shape of anomaly is counterintuitive. Since below YBCO is a layer of LCMO, one would expect decrease of resistance of the bilayer below  $T_{Curie}$ , where  $R$  of LCMO suddenly drops. Instead, resistance is increasing. It indicates that charge carriers have difficulties of overflowing from LCMO to YBCO at temperatures below  $T_{Curie}$ . This is effect of spin injection from LCMO into normal state of YBCO, which is not paid attention to or ignored in the literature, but which is as remarkable as spin injection into superconducting state of YBCO. Indeed, above  $T_{Curie}$  about half of electrons have spin up and half spin down both in YBCO and LCMO, so there is no energy cost for the them to overflow from one material to another. In contrast, below  $T_{Curie}$ , half of electrons are of spin up and half of spin down in YBCO, but in LCMO all electrons have spin up, and there is energy cost for changing spin population when overflowing between the materials.

One would expect that situation will change if current is not injected from LCMO to YBCO, but simply flows between different parts of YBCO, for example, when it passed through contacts  $I_1$  and  $I_2$ . Indeed, in this case increase in resistance does not take place. A comparison between two cases is given in Fig. 6 for a set of load voltages shown in the legend in inset. Bold curves are for current between  $I_1$  and  $I_3$ , and thin curves are for current between  $I_1$  and  $I_2$ . For a better comparison, a linear curve is subtracted from each set of data. Black arrows indicate beginning of spin polarization transition, while red arrows show position of maximum or minimum in resistance, which develop in presence or absence of spin injection, respectively.



**Figure 6:** Temperature dependence of resistance for the sample in Fig. 1 with current flowing between contacts  $I_1$  and  $I_3$  (bold lines) and between contacts  $I_1$  and  $I_2$  (thin lines). The voltage is measured between contacts  $V_1$  and  $V_2$ . A linear curve is subtracted from each set of data recorded at the same varied voltage loads shown in the legend.

The same technique of changing position of current leads, but keeping potential leads at the same contacts, i.e. injecting spin-polarized electrons or just passing current mainly in YBCO, can be used to demonstrate effect of spin injection on superconducting state of YBCO. Fig. 7 shows temperature dependence of the resistance of YBCO, measured between contacts  $V_1$  and  $V_2$ , in the vicinity of the superconducting transition. In this experiment, current is passed through the contacts  $I_1$  and  $I_3$  (black curves) or  $I_1$  and  $I_2$  (red) at four voltage loads of 1, 3, 9 and 15 V. Black curves represent case of forceful spin injection, while red curves correspond to current mainly flowing in YBCO (some overflow of current to LCMO is still possible). It is clear that spin injection strongly affects superconducting transition and its influence increases with increase of the voltage load.

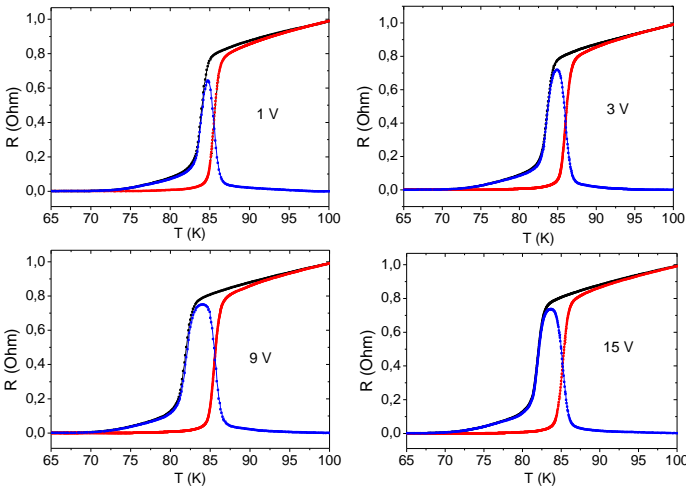


**Figure 7:** Temperature dependence of the resistance of YBCO measured between contacts  $V_1$  and  $V_2$  in the vicinity of superconducting transition, for the current flowing through the contacts  $I_1$  and  $I_3$  (black curves) and  $I_1$  and  $I_2$  (red). Curves are for four values of voltage load from 1 to 15 V shown in subplots.

Blue curves in Fig. 7 are the difference curves between black and red lines. These curves show the addition resistance due to the spin injection. One can see that effect of spin injection is strongest just below  $T_c$ , where superconductor is relatively weak. The addition resistance is overlapped with red curves resulting in the apparent shift of superconducting transition. Such a behavior explains additional resistance peak observed in [9]. One of the curves showing this peak is plotted in Fig. 8.

The sample in [9] was prepared ex-situ, i.e. deposition of LCMO above YBCO took place after removing sample from the deposition chamber. Due to modification of interface in air,  $T_{Curie}$  of LCMO shifted to temperature below  $T_c$  of YBCO. At the decrease of temperature, first superconducting transition takes place with corresponding drop in resistance at about 90 K. After that, spin-polarization transition starts in LCMO forming the peak similar to that shown by blue curves in Fig. 7. It is important to note that such peak can only be seen if  $T_{Curie}$  is close to  $T_c$ .

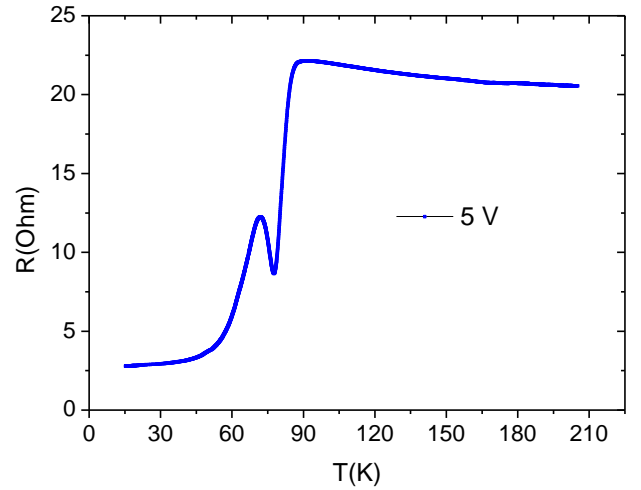


**Figure 8:** Temperature dependence of resistance for an ex-situ LCMO/YBCO bilayer showing peak effect below superconducting transition.

To extend the above activity to quantum superconducting circuits expected to operate at high temperatures, a combination of YBCO and LCMO with graphene [4] needs to be explored. In this paper, the latter was taken in form of nano-plates in a water solution. A drop of the solution was first deposited to YBCO covering its whole area between contacts  $V_1$ ,  $V_2$ ,  $I_1$  and  $I_2$ . It was quickly dried to avoid possible interaction of YBCO with water. The result, however, was nearly complete suppression of superconducting transition, as it is shown in Fig. 9 in semi-logarithmic scale. The resistance measured between  $V_1$  and  $V_2$ , with current flowing between  $I_1$  and  $I_2$ , increases more than one order of magnitude exposing the resistance of LCMO below YBCO with its characteristic drop at  $T_{Curie}$  of about 250 K.

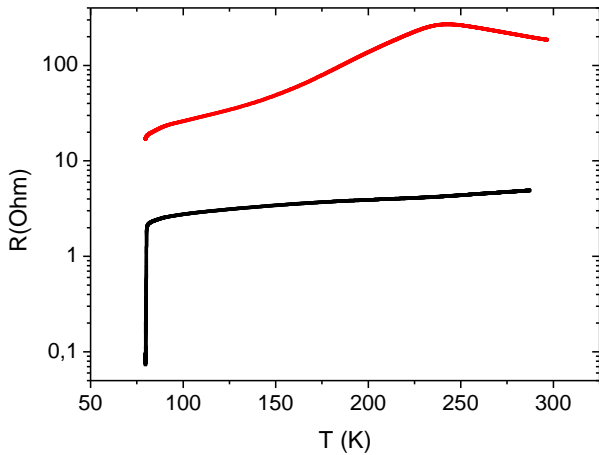


**Figure 9:** Temperature dependence of the resistance of YBCO measured between contacts  $V_1$  and  $V_2$  after deposition of the layer of graphene (red curve) and before the deposition (black curve). The current is flowing between contacts  $I_1$  and  $I_2$ . The axis of resistance is in the logarithmic scale.

In contrast to YBCO, the influence of graphene on LCMO is very moderate. In Fig. 10, temperature dependence of the resistance of LCMO in the uncovered by YBCO area is shown before the deposition of graphene (black curve), after the deposition of first graphene layer (red curve) and the second layer (green curve). The first layer of graphene only slightly increases resistance of LCMO not shifting  $T_{Curie}$ . Second layer slightly shifts  $T_{Curie}$  to a lower temperature. A small decrease in resistance comparable with red curve is also registered for the green curve, which is probably due to contribution of the conductance of graphene.

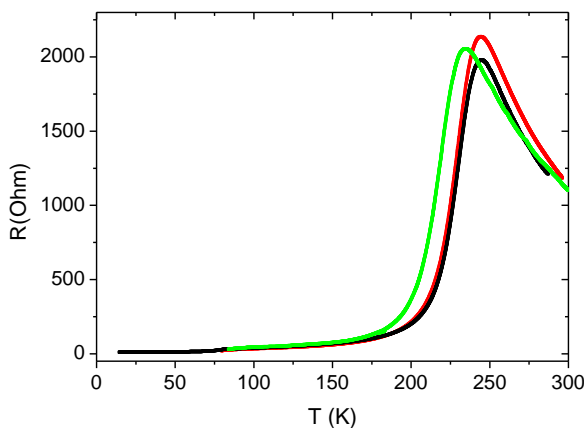


**Figure 10:** Temperature dependence of the resistance of LCMO in the uncovered by YBCO area before the deposition of graphene (black curve), after the deposition of first graphene layer (red curve) and the second layer (green curve).

In the experiments with graphene, it appears to be very harmful for YBCO. The influence of water still cannot be excluded, and the non-water solutions of graphene nanoflakes should be tried. The influence of graphene on LCMO is very moderate.

#### IV. SUMMARY

A detailed study of in-situ YBCO/LCMO bilayer by electrical transport measurements in wide range of temperatures has been performed using an array of current and potential leads in the sample partially covered by YBCO. Effect of spin injection from LCMO on normal and superconducting state of YBCO was clearly demonstrated, and unusual peak in resistance appearing below superconducting transition of YBCO in ex-situ sample has been explained. The influence of graphene on YBCO and LCMO was investigated showing that graphene can be extremely harmful for YBCO, but its influence on LCMO is very moderate.

#### REFERENCES

- [1] D. Castelvecchi, "Quantum cloud goes commercial," *Nature*, vol. 543, p. 159, March 2017.
- [2] J. Linder and J.W.A. Robinson, "Superconducting spintronics," *Nat. Phys.*, vol. 11, pp. 307-315, August 2015.
- [3] Y.-P. Shim and C. Tahan, "Semiconductor-inspired design principles for superconducting quantum computing," *Nat. Commun.*, vol. 7, pp. 11059, March 2016.
- [4] A.K. Geim, K.S. Novoselov, "The rise of graphene," *Nature Materials*, vol. 6, pp. 183-191, March 2007.
- [5] R. Werner, C. Raisch, A. Ruosi, B. A. Davidson, P. Nagel, M. Merz, S. Schuppler, M. Glaser, J. Fujii, T. Chassé, R. Kleiner, and D. Koelle., "YBa<sub>2</sub>Cu<sub>3</sub>O<sub>7</sub>/La<sub>0.7</sub>Ca<sub>0.3</sub>MnO<sub>3</sub> bilayers: Interface coupling and electric transport properties," *Physical Review B*, vol. 82, 224509, December 2010.
- [6] N.C. Yeh, R. P. Vasquez, C. C. Fu, A. V. Samoilov, and K. Vakili, "Nonequilibrium superconductivity under spin-polarized quasiparticle currents in perovskite ferromagnet-insulator-superconductor heterostructures," *Physical Review B*, vol. 60, pp. 10522-10526, 1999.
- [7] P. Mikheenko, M.S. Colclough, C. Severac, R. Chakalov, F. Wellhoffer and C.M. Muirhead, "Effect of spin-polarized injection on the mixed state of YBa<sub>2</sub>Cu<sub>3</sub>O<sub>7-δ</sub>," *Appl. Phys. Lett.*, vol. 78, pp. 356, November 2001.
- [8] S.Soltan, J. Albrecht, and H.-U. Habermeier, "Transport properties of LCMO/YBCO hybrid structures," *Materials Science and Engineering B*, vol. 144, pp. 15-18, 2007.
- [9] A.S. Fjellvåg, T.B. Hjelmeland, H.J. Mollatt, T. Qureshiy, P. Mikheenko, "Interplay between spin polarization and superconductivity in an ex-situ bilayer La<sub>0.67</sub>Ca<sub>0.33</sub>MnO<sub>3</sub> - YBa<sub>2</sub>Cu<sub>3</sub>O<sub>7-x</sub>," In *Proceedings of the 2017 IEEE 7th International Conference on Nanomaterials: Applications & Properties (NAP-2017)*. IEEE. ISBN 978-1-5386-2810-2. Part 2, pp. 02NTF02-1 - 02NTF02-5, 2017.